The solar EUV and X-rays as ionizing source for planetary atmospheres

B. N. Dwivedi

Department of Applied Physics, Institute of Technology, Banaras Hindu University, Varanasi 221 005, India

The current knowledge of the solar spectral irradiance at the EUV and X-ray wavelengths has been presented and emission processes detailed. Observational data and their importance in the analysis of the photochemistry and energy balance of the planetary atmospheres and in probing the solar plasma have been highlighted. The current ideas and problems about the effects of specific solar features on the variability of the spectral irradiance have also been briefly discussed.

THE Sun having the photospheric temperature of 6000 K was not expected to support an extended outer atmosphere or produce EUV and X-ray emission. Hulburt (1938) for the first time predicted that 'ultraviolet light, X-rays or particles of zero average charge' must be responsible for the formation of the E-layer of the earth's ionosphere. This speculative theory was further supported by earlier observation of Grotrian[1] in 1931 who drew attention to the smearing out of the Fraunhofer lines after scattering by coronal electrons. In 1942, Edlen[2] identified the magnetic dipole transitions in highly ionized iron observed in the visible spectrum of the solar corona during eclipses. The existence of these ions in the coronal gas led to the discovery of million degree hot corona. (The electron temperature as a function of height in the solar atmosphere is shown in Figure 1 for illustration.) At this stage, the study of solar EUV and X-ray emission became imperative. However, further study had to await the availability of vehicles to carry instruments above the absorbing layers of the earth's atmosphere. The US Naval Research Laboratory (NRL) under E.O. Hulburt first began the observational study in 1946, using V-2 rockets. The first detection of solar X-rays was made on 6 August 1948 by the NRL group[3] and the first ultraviolet solar spectrum down to 240 nm was recorded at 55 km altitude on 10 October 1946[4]. Since then there is a bewilderingly large amount of EUV and X-ray data available from various balloon, rocket and satellite measurements.

The major problem in correlating all the available data on solar EUV and X-ray spectrum arises because of the divergence of interests between solar physicists and aeronomers. The primary objective of aeronomy is to find out the reliable EUV data with maximum photometric accuracy for a quantitative understanding of the physical phenomena taking place in the upper atmosphere. On the other hand, the primary interest of the solar physicists is to increase the spatial and spectral resolution of the X-ray and EUV instrumentation in order to optimize the fine structure of the solar disk. The solar physicists may, therefore, consider earth's atmosphere as an obstacle. Nevertheless, it is advisable to know the structure and behaviour of an obstacle if one wants to avoid it.

Generation of solar X-rays and EUV radiation

The physical processes that produce solar X-ray, EUV and UV radiation are mainly emission and absorption continua and lines. Depending on the wavelength region of the spectrum, one considers the importance of physical processes which account for the generation of the radiation from the solar atmosphere. Figure 2 depicts an illustrative view of the occurrence of highly ionized atoms in the solar atmosphere vividly describing the regions from which line emission from these atoms is generated. A great deal of information about the state of plasma especially electron density, temperature and emission measure can be obtained from the line and continuous spectra of the solar corona. The theoretical understanding of the processes is needed to compare with observational data. Corona is not in local thermodynamic equilibrium (LTE). Neither the ionization balance, the level population, nor the radiation field may be computed from the familiar equations of thermal equilibrium.

Ionization balance

In the normal solar corona, the dynamic equilibrium exists between electron collisional and auto-ionizations on one hand and radiative and dielectronic recombinations on the other. The ratio of the concentration of the ith species to that of the $(i+1)^{th}$ is given by

$$\frac{N_i}{N_{i+1}} = \frac{\alpha_R + \alpha_D}{q_e + q_A}$$

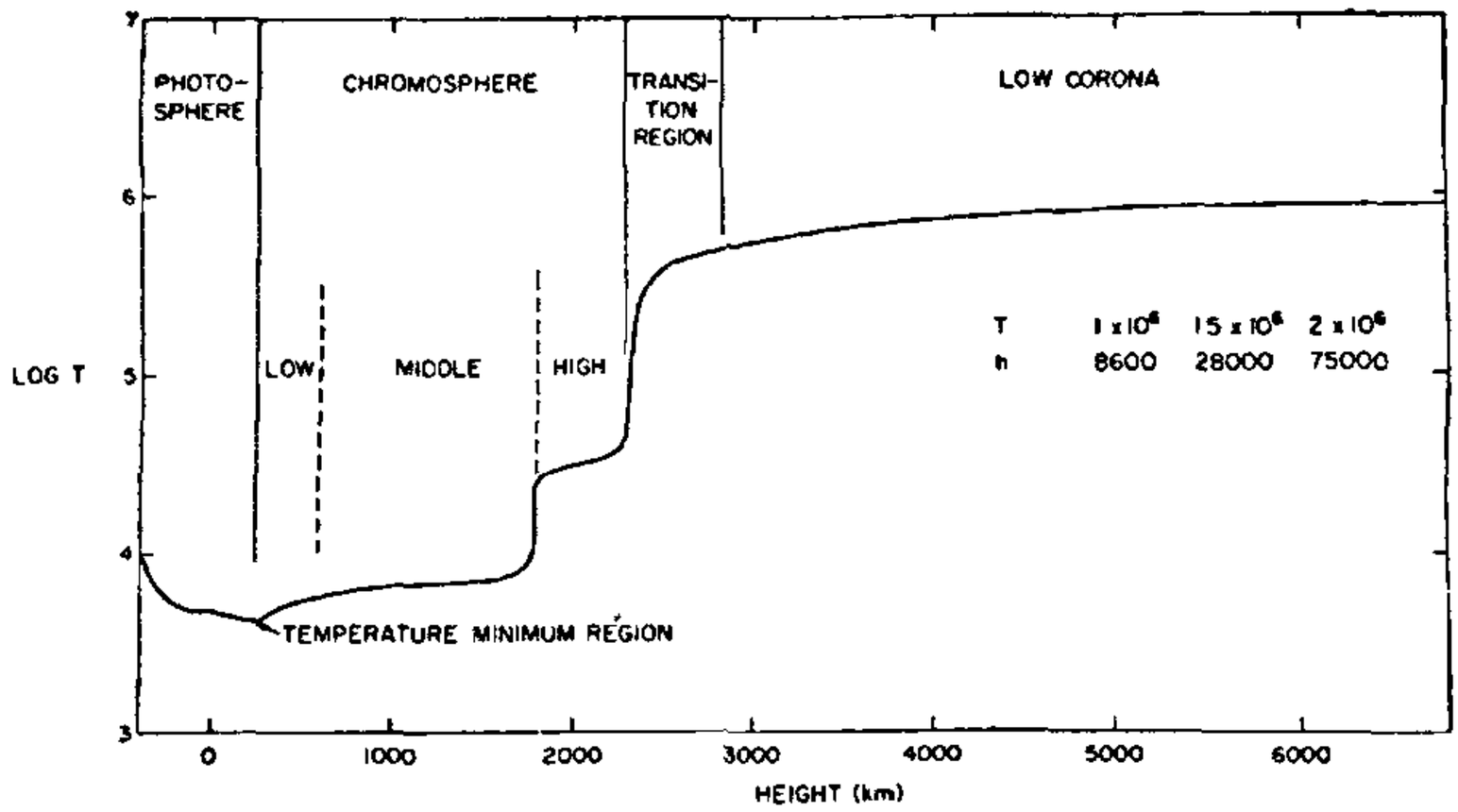

Figure 1. Temperature distributions in the chromosphere-corona interface (from Goldberg[31])

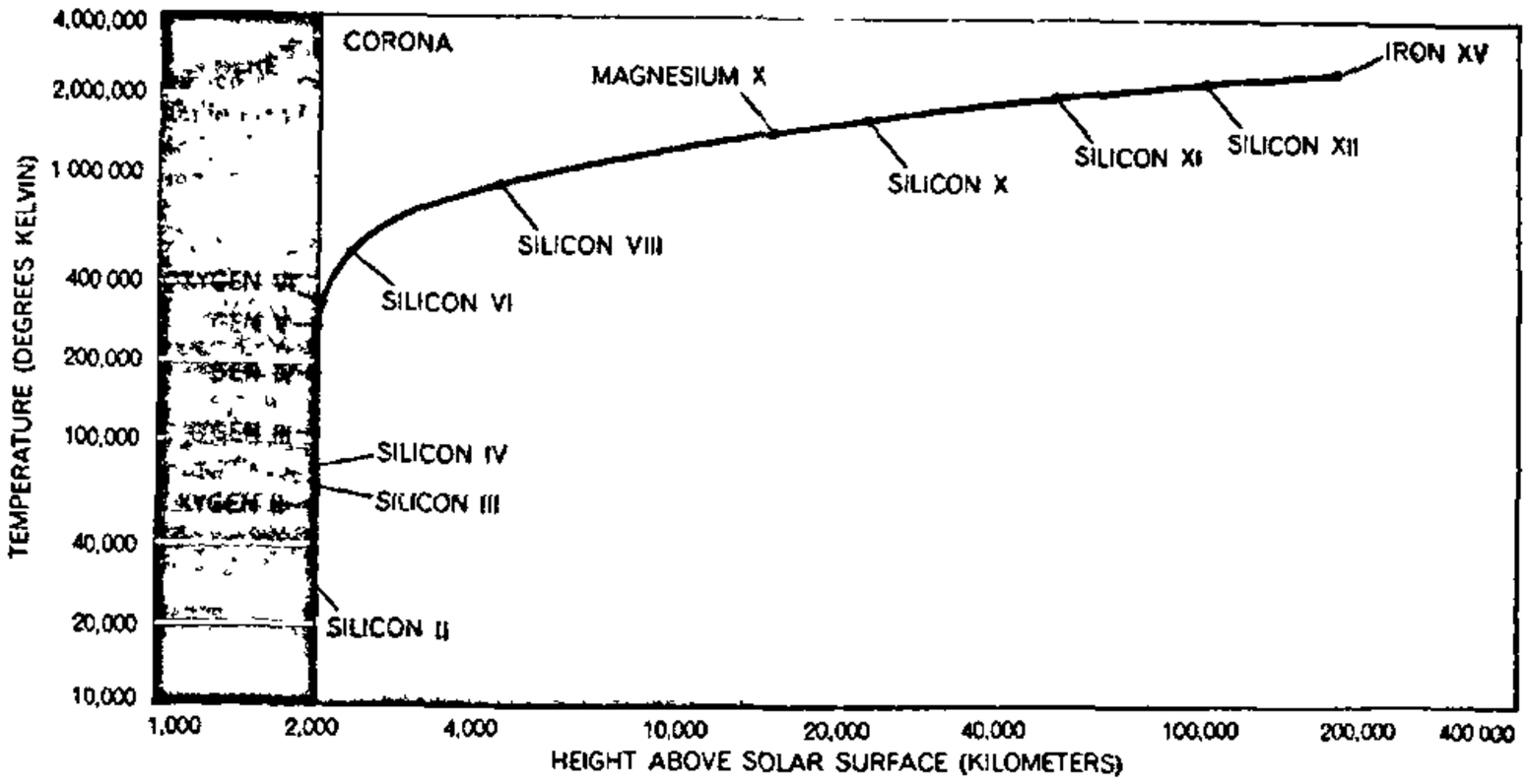

Figure 2. Location of various stages of ionization (from Goldberg[31]).

$$= \frac{\text{Radiative} + \text{Dielectronic recombination rate}}{\text{Electron collisional} + \text{Auto-ionization rate}}$$

From a knowledge of the process rates, the fraction N_{ion}/N_{el} as a function of electron temperature can be calculated by the repeated use of the above equation. This has been done by Jordan[5] and more recently by Arnaud and Rothenflug[6] for the most abundant coronal elements.

Continuum emission

Knowing the plasma ionization balance, the intensity of the emitted radiation as a function of wavelength and temperature can be calculated. The three significant continuum emission processes are:

(1) Bremsstrahlung or free-free radiation from thermal plasma (Coulomb scattering of electrons by ions).
(2) Radiative recombinations of electrons and ions or free-bound radiation.
(3) The two-photon decay of certain metastable levels of helium and hydrogen like ions.

For the detailed formulae and theoretical calculations of continuum emissions, the reader is referred to the work of Tucker and Koren[7], and Kato[8].

Line emission

The analysis and interpretation of line emission provide detailed information on the physical conditions of the coronal plasma. The line emissivity (per unit volume, per unit time) for an optically thin spectral line is given by

$$\varepsilon(\lambda_{ij}) = N_j A_{ji} hc / \lambda_{ji},$$

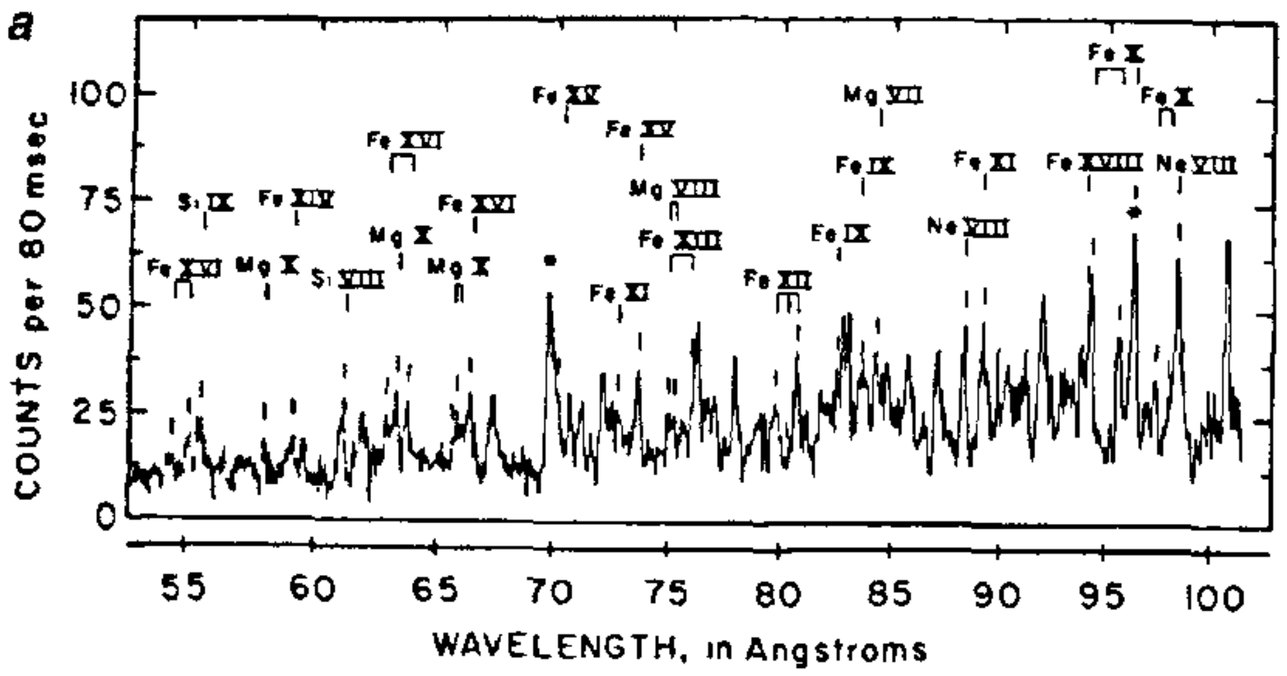

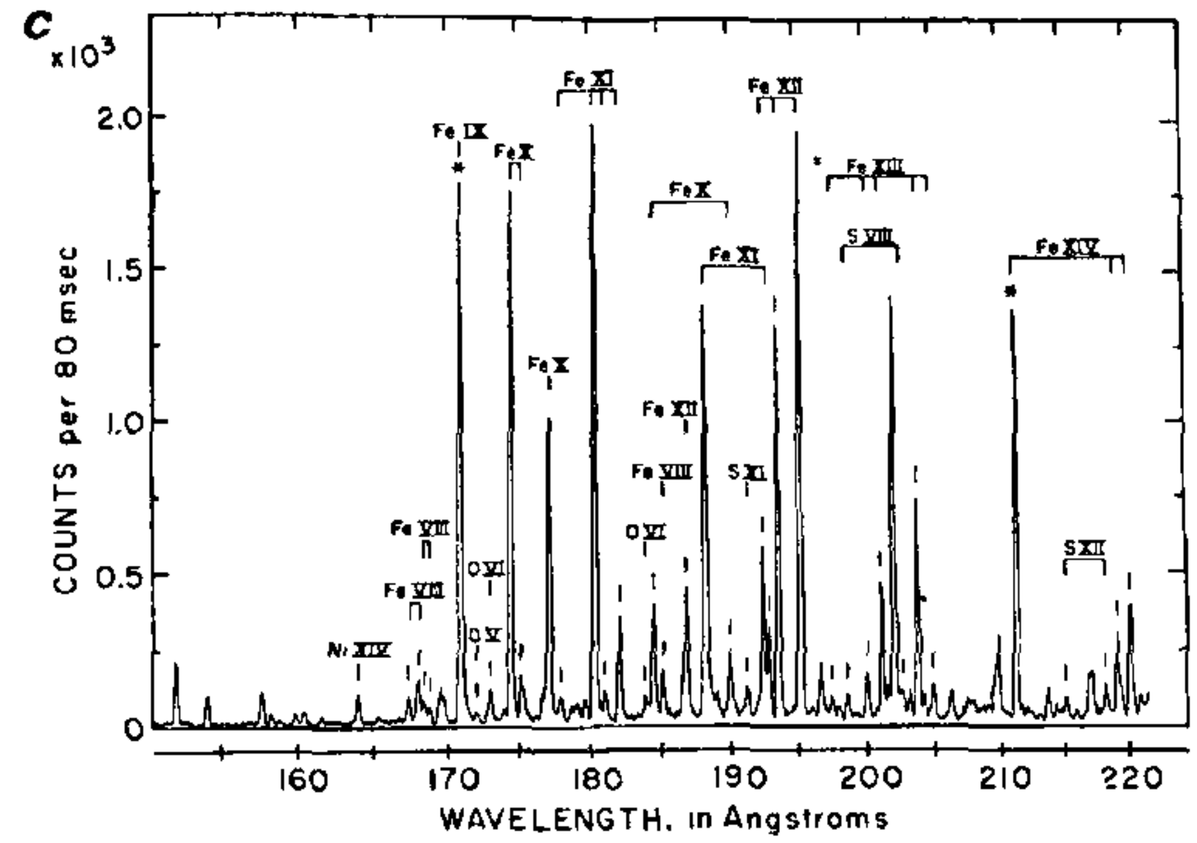

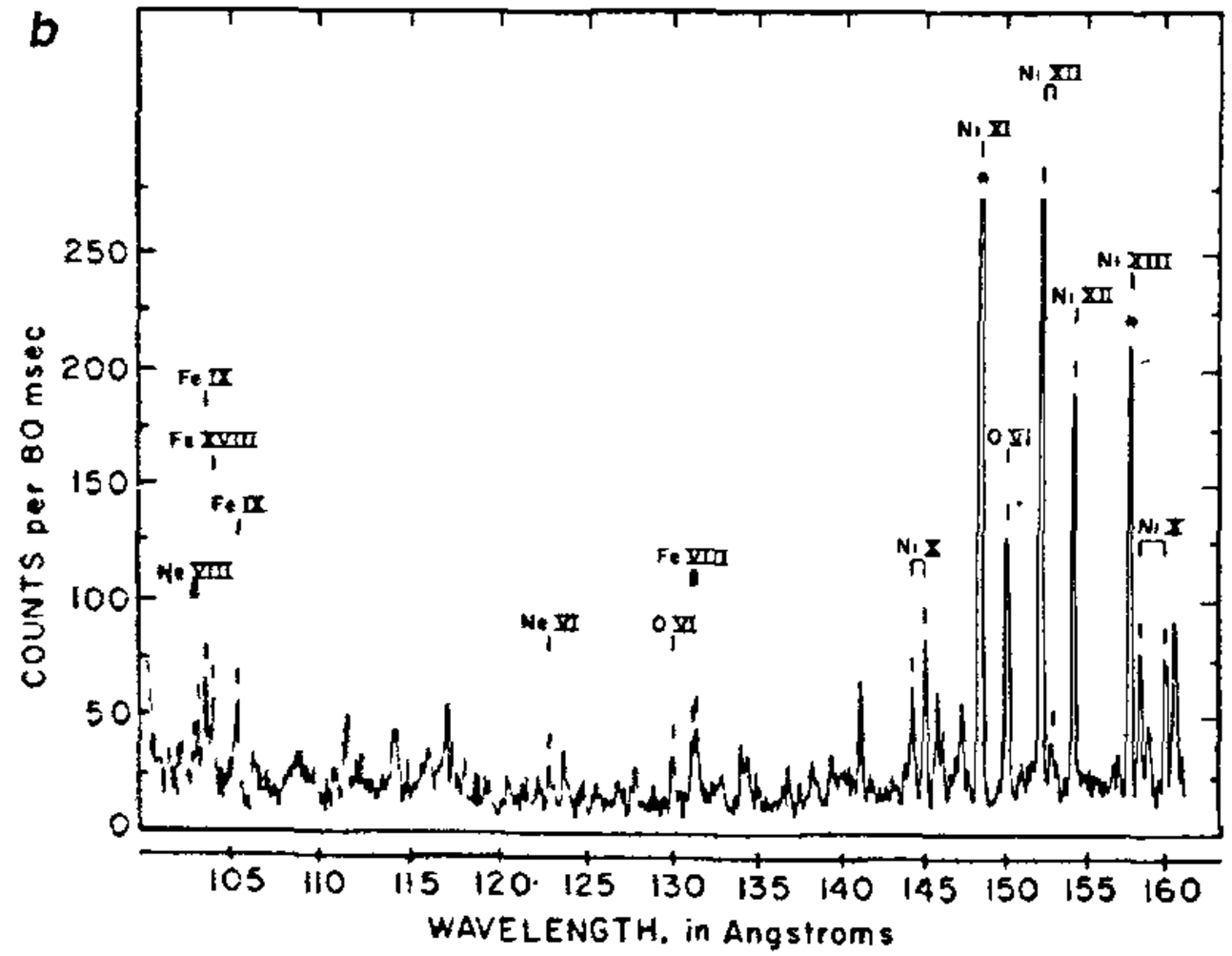

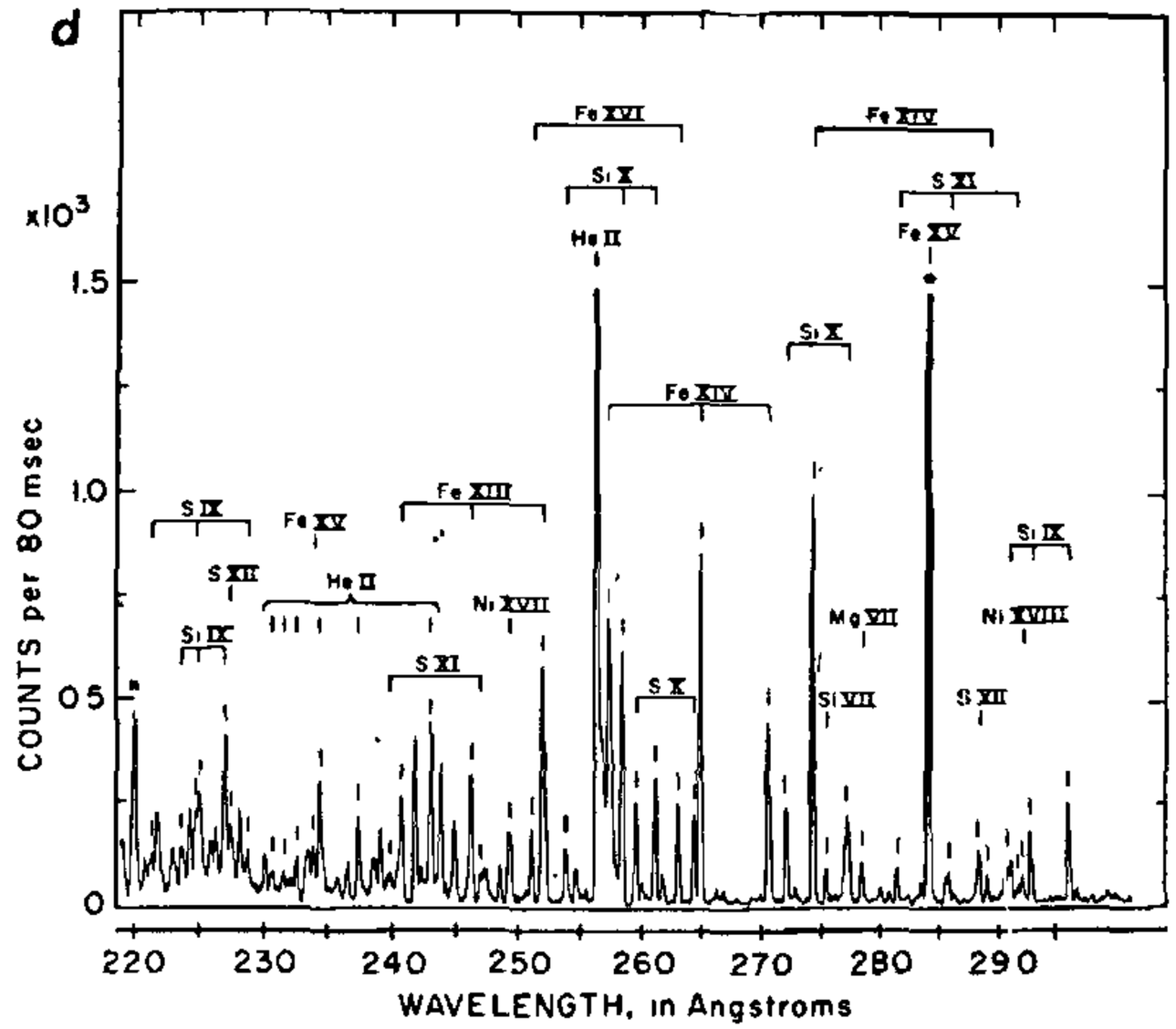

Figures 3*a–d*. The spectrum between 55 Å and 300 Å of the entire solar disk obtained at 1935 UT on 4 April 1969. The asterisks indicate the reference lines used to obtain the wavelength scales (from Malinovsky and Heroux[14])

where A_{ji} is the spontaneous transition probability and N_j the number density of the upper level j.

$$N_j = \frac{N_j(X^{+p})}{N(X^{+p})} \cdot \frac{N(X^{+p})}{N(X)} \cdot \frac{N(X)}{N(H)} \cdot \frac{N(H)}{N_e} \cdot N_e.$$

Here $N(X^{+p})/N(X)$ is the ionization ratio of the ion X^{+p} relative to the total number density of element and is primarily a function of electron temperature; $N(X)/N(H)$ is the element abundance which may or may not be constant in the solar atmosphere; $N(H)/N_e$ is the hydrogen abundance which is usually assumed to be around 0.8; N_e is the electron number density; $N_j(X^{+p})/N(X^{+p})$ is the population of level j relative to the total number density of the ion X^{+p} which is a function of electron density and temperature and is determined by solving the statistical equilibrium equations for the ion accounting for various physical processes that are significantly involved.

For the detailed formulae and theoretical calculations of solar emission lines, the reader is referred to the work of Gabriel and Jordan[9], Dere and Mason[10], Dwivedi[11–13] and references cited therein.

Solar radiation for aeronomical studies

For the sake of simplicity, the observed solar X- and EUV radiation is shown below 1300 Å, the range covered in this review. From 55 Å to 300 Å the results (Figures 3*a–d*) are taken from the observed spectrum of Malinovsky and Heroux[14], whereas for the range 280 Å to 1350 Å the skylab observations (Figures 4*a–c*) are taken from Vernazza and Reeves[15]. The calculated spectrum by Kato[6] in the range of 1 Å to 100 Å is shown in Figure 5. These figures show the complexity of the emission processes that one has to deal with in order to explain the spectrum. However, our purpose is to discuss their use for aeronomy.

For wavelengths < 4 Å, the line emission is not dominant. For solar radiations below 1200 Å, the spectrum is dominated by the chromospheric, transition region and coronal emission lines with a few weak emission continua as is evident from Figures 3 and 4. This radiation is the dominant source of energy for heating and ionization in the terrestrial upper atmosphere at an altitude above 90 km. The photoionization limits for the major neutral constituents O_2, O and N_2 of the terrestrial atmosphere occur at wavelengths 1027 Å, 911 Å and 796 Å respectively. The radiation, 911 Å to 1200 Å, is absorbed mainly by O_2 with, 911 Å to 1027 Å, contributing a large fraction of available energy for ionization in the E-region at altitudes 100 km to 150 km. The radiation, 911 Å–796 Å, is absorbed both by O_2 and N_2 whereas the absorption by O dominates at the radiation below 796 Å. The radiation, 911 Å–300 Å, provides the bulk of energy for ionization of three major neutral species in the F-region of the ionosphere (150–400 km). A knowledge of solar EUV spectral irradiance is, therefore, of crucial importance in any analysis of the photochemistry and energy balance of the ionosphere and thermosphere.

The solar EUV spectrum contains well-separated emission lines of the atoms of the astrophysically abundant elements superimposed on relatively weaker continua of H, He, C and Si. To longer wavelengths 1200 Å–2000 Å spectrum is primarily continuum emission from the lower chromosphere and upper photosphere, with superimposed chromospheric emission lines and some absorption lines. For wavelengths greater than 2000 Å, the solar spectrum is primarily continuum radiation from the photosphere with a multitude of superimposed absorption lines and continua. In the terrestrial atmosphere the solar radiation 1250 Å–2000 Å is absorbed in the lower thermosphere and mesosphere by O_2 yielding atomic oxygen. The solar radiation 2000 Å–3000 Å is absorbed in the upper and lower stratosphere and is responsible for the photochemistry of the stratospheric ozone.

The EUV spectral region is well-suited for the quantitative study and modelling of a wide range of solar structures from features associated with intense solar activity through the regions of quiescent atmosphere to coronal holes. Line intensity ratios provide T_e and N_e diagnostics of solar plasma (refer Gabriel and Jordan[9], Dere and Mason[10], Dwivedi[11, 13] and references cited therein).

Solar spectral irradiance

The solar spectral energy distribution is usually given in terms of either spectral irradiance at the centre of the solar disk (ergs sec^{-1} cm^{-2} A^{-1} sr^{-1}) or spectral irradiance of the whole Sun at 1 AU. Because of limb-darkening (or brightening at short wavelengths) and increased brightening in active regions, the radiance is not uniform at all points on the disk. The relation between the average spectral radiance of the disk L_λ and that at the disk centre $L_{\lambda c}$ is

$$L_\lambda = L_{\lambda c} \int_0^{\pi/2} R_{\lambda\theta} \sin\theta \cos\theta \, d\theta,$$

where θ is the angle subtended at the centre of the Sun by two solar radii, one passing through the disk centre and other passing through any other surface element on the Sun and $R_{\lambda\theta}$ is the limb-darkening (or brightening) function. The spectral irradiance E_λ of the Sun at 1 AU is given by the expression

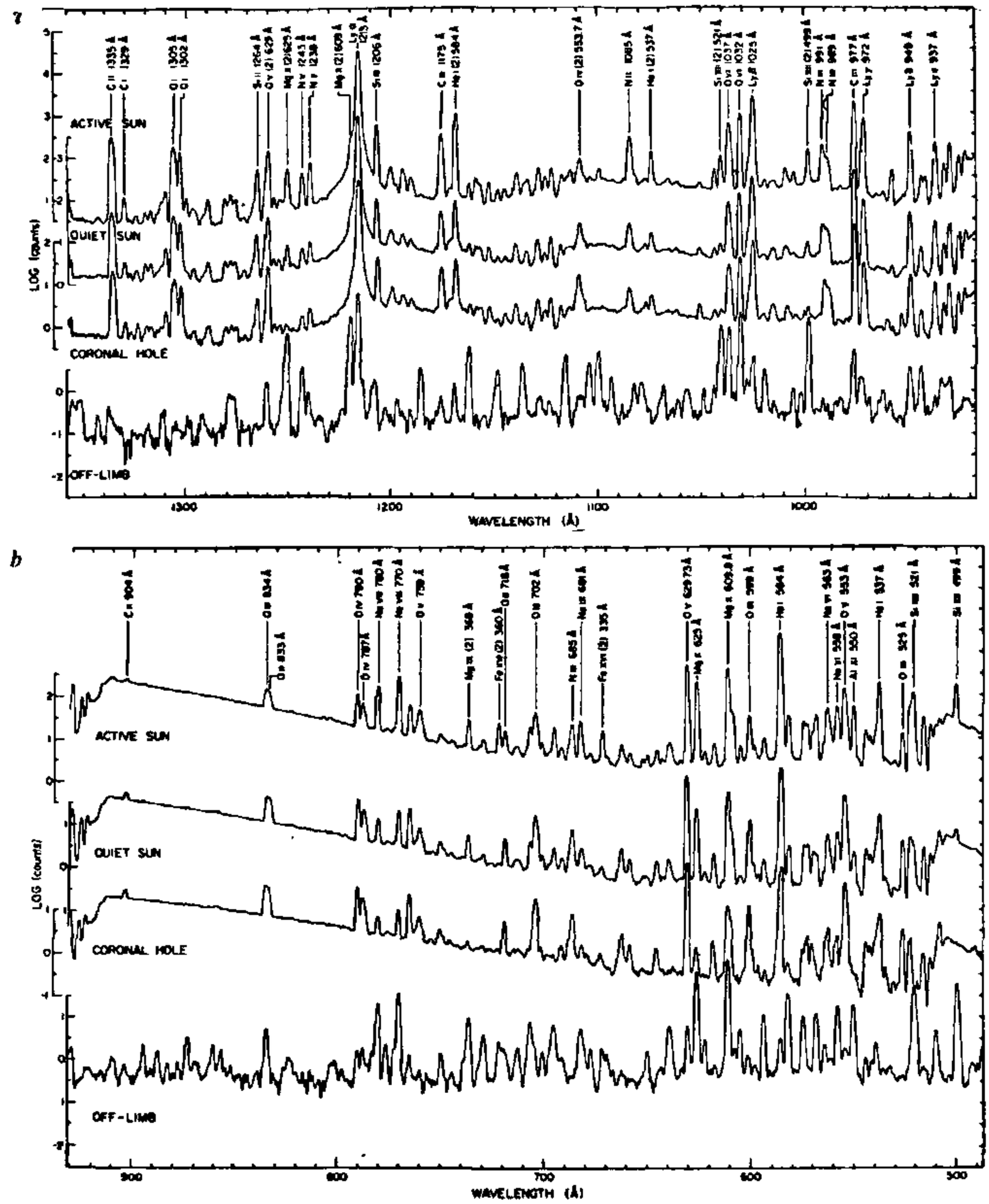

Figures 4 *a–c*. Average solar spectra between 1350 Å and 280 A of a quiet area, a coronal hole, an active region and a quiet area off the limb The individual spectra have been displaced two decades from each other for clarity (from Vernazza and Reeves[15])

$$E_\lambda = 2\pi \left[\frac{r}{R}\right]^2 L_\lambda \int_0^{\pi/2} \sin\theta \cos\theta \, d\theta$$

$$= \pi \left[\frac{r}{R}\right]^2 L_\lambda = 6.7997 \times 10^{-5} L_\lambda,$$

where r is the solar radius and R is 1 AU. The total irradiance E, or the solar constant, is given by the expression

$$E = \int_0^\infty E_\lambda \, d\lambda.$$

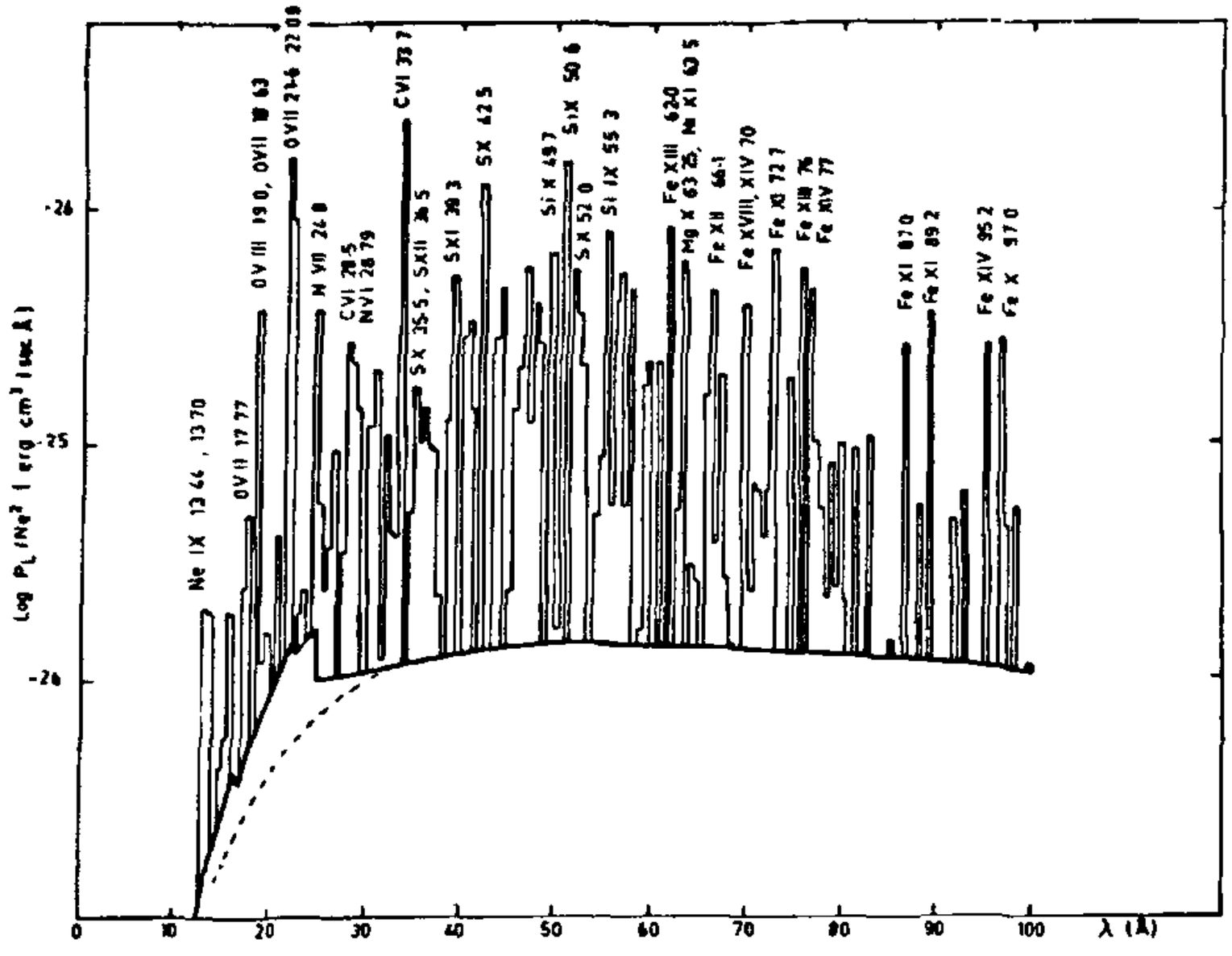

Figure 5. The computed spectrum of a hot thin plasma at 1.6×10^6 K in the wavelength range 1 Å–100 Å. The bremsstrahlung emission is indicated by dashed line and the solid line shows the sum of bremsstrahlung and recombination radiation. Some intense lines are labelled according to ion and wavelength (from Kato[8])

The understanding of solar EUV irradiance variability is a prerequisite for aeronomy[16] and for climate research[17] and is essential if perturbations of anthropogenic origin are ever to be extracted from the long-term records of atmospheric parameters[18].

Solar irradiance variability

During the high solar activity and flares, solar X-radiation is enhanced affecting the ionospheric D-region. The results of measurements aboard Synchronous Meteorological Satellites (SMS-1 and 2), Geostationary Operational Environmental Satellite (GOES-1) are available. The X-ray variability exceeds five orders of magnitude on a solar cycle time scale. It changes by two orders of magnitude during flares on a time scale of seconds[19]. Little is known about 25 Å–150 Å variability. However, the radiation 150 Å–1200 Å is important for aeronomy of the upper atmosphere and hence for satellite orbit prediction.

The tabulation of solar EUV flux is given by Hinteregger *et al.*[20]. Though some variability of the flux was expected from the observations of OSO-1, no estimate could be presented. The tabulation of Hinteregger *et al.*[20] was used as 'EUV standard flux' for many years. However, EUV spectrometer aboard OSO-3 in 1967[21], and 304 Å monochromator aboard OSO-4 in 1967 and 1968[22] showed the EUV flux variability distinctly. Twenty-five per cent variations in the flux were observed in the short term (5–10 min) and 40% variations in the medium term (solar rotation) time scale.

Extensive data are available during solar cycle 21. Measurements by EUVS on the AE-E satellite are reported by Hinteregger *et al.*[23]. The EUV flux in the 100 Å–1210 Å range observed by AE-E satellite from 1976 to 1980, the ascending period of the solar cycle 21, have been discussed[24–26]. However, the temporal variation and the magnitude of its variability has been questioned on the basis of linear correlation analysis with 10.7 cm radio flux[27, 28]. The uncorrected AE-E radiances appear to be consistent with He^+ abundance and He 10830 Å. In the quiet Sun the 2800 MHz flux originates at the transition region altitudes with temperature of the order of 8×10^5 K while in active regions with high plasma densities, the emission originates at higher altitudes in the corona where the temperature is 10^6 K or greater. Consequently the irradiances of coronal EUV lines can be expected to track the radio flux more closely than the irradiances of chromospheric or transition-region lines. One therefore concludes 'the 2800 MHz radio noise index is unreliable indicator of the magnitude of the EUV irradiance and should be replaced by direct measurements at EUV wavelengths on a routine basis'.

Just as in 1976, in the beginning of solar cycle 21, it was anticipated that the data acquired in that cycle

would finally provide definite information about solar UV irradiance variations during the solar cycle; so too, the results of new measurements of the current cycle 22 and their interpretations would be of great scientific value.

Impact of solar flares

The electromagnetic radiation and particle emissions are considerably enhanced during solar flares. The following effects are generally associated with the occurrence of flares:

1. Enhanced X-rays and EUV radiation,
2. Protons, α-particles and electrons,
3. Energized solar wind plasma leading to magnetic storm.

The impact of solar flares with regard to their enhanced X-rays and EUV radiation will be briefly discussed here. Solar particle effects are outside the purview of this article.

EUV and X-ray effects

The EUV and X-ray enhancements are highly variable. 2 Å–10 Å emission can rise by several orders of magnitude. In the same flare Lyman-α (1216 Å) might increase by a few per cent. The enhanced X-ray and EUV radiation immediately (little over 8 minutes after the event) affect the D, E and F regions of the sunlit ionosphere. The E and F regions are mainly affected by EUV radiation whereas X-rays significantly affect the D-region (< 100 km) of the ionosphere. In addition to chemical changes, the X-ray and EUV enhancements cause dynamical effects. The large enhancements in conductivity due to increased ionization have been found to excite MHD waves in the magnetosphere[29].

Radio communications

Radio wave propagation is affected extensively by the changes in the ionospheric electron density N_e profile as shown in Figure 6. SIDs collectively describe a number of irregular and impulsive events which affect the intensity, frequency and phase of radio signal. The long-range transpolar transmissions at very low frequencies (VLF), used for navigation and military communications, may be severely disturbed. Also, civil and military communications at HF may suffer black-outs for many hours in a large SPE. An increase in ionization can produce anomalously long-path propagation of signals which are intended to be only local. The nuisance aspect of the phenomena is real.

The distress calls from the crash of a small plane in west Virginia in February 1979 were heard in Orange county, California, causing a considerable confusion in the local civil emergency procedures[30]. Such events as these are not isolated during intervals of solar storminess and are certainly a problem to the people and institutions concerned.

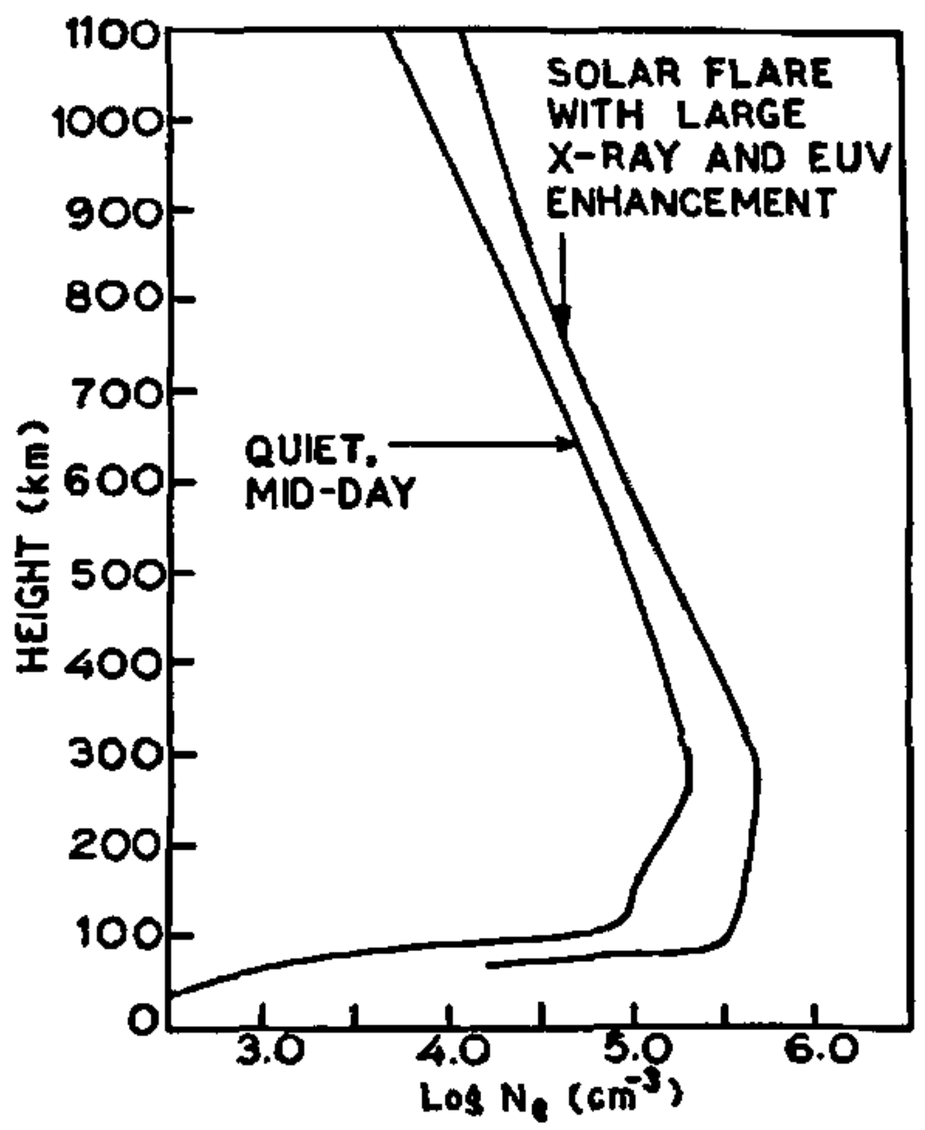

Figure 6. Typical electron densities in the quiet daytime ionosphere with those produced by the enhanced X-ray and EUV emissions of a large solar flare

Conclusion

Solar EUV and X-rays, their variability and consequent impact on the planetary atmospheres constitute a problem that needs a definite answer. This is a challenging task and only continuous monitoring in space on a long-time scale, can be a way out. Indirect measurements will not provide a definitive answer. On the other hand, the solar physicists and aeronomers together could coordinate their observations to achieve the desired results.

1 Grotrian, W, *Z Astrophys*, 1931, **3**, 199
2 Edlen, B, *Z Astrophys*, 1942, **22**, 30
3 Burnight, T. R, *Phys Rev*, 1949, **76**, 165
4. Baum, W. A, Johnson, F S, Oberly, J. J, Rockwood, C C, Strum, C. V and Tousey, R, *Phys Rev*, 1946, **70**, 781–782
5 Jordan, C, *Mon Not R astr Soc*, 1969, **142**, 501–521
6 Arnaud, M and Rothenflug, R, *Astr Astrophys Suppl Ser*, 1985, **60**, 425–457
7 Tucker, W. H and Koren, M, *Astrophys J*, 1971, **168** 283–311
8 Kato, T, *Astrophys J Suppl Ser*, 1976 **30** 397–419
9 Gabriel, A H and Jordan, C, in *Case Studies in Atomic Collision Physics II* (eds McDaniel I W and McDowel, M R C), North Holland, 1972, pp 210–291

10 Dere, K. P and Mason, H E., in *Solar Active Region* (ed. Orrall, F Q), Colorado Univ Press, 1981, pp 129–164.
11 Dwivedi, B N , *Kodaikanal Obs Bull* , 1988, **9**, 99–110
12 Dwivedi, B N , *Sol Phys Lett* , 1989, **122**, 185–188
13 Dwivedi, B N , *Adv Space Res* , 1991, **11**, 303–306.
14 Malinovsky, M and Heroux, L., *Astrophys J.*, 1973, **181**, 1009–1030.
15 Vernazza, J E. and Reeves, E. M , *Astrophys. J. Suppl. Ser* , 1978, **37**, 485–513
16 Kockarts, G , *Sol Phys* , 1981, **74**, 295–320.
17 National Academy of Sciences, *Studies in Geophysics: Solar Variability, Weather and Climate*, National Academy Press, Washington, D C., 1982
18 Wuebbles, D J , in Proceedings of the quadrennial ozone symposium (ed Zerefos, C. S and Ghazi, A), D. Reidel, 1985, pp 87–91
19 Keplin, R. W., Dere, K P., Horan, D M and Meekins, J. F., in *Solar Output and its Variation* (ed White, O R), Colorado Associated Press, 1977, pp. 287–312.
20. Hinteregger, H E , Hall, L A. and Schmidtke, G , *Space Res* , 1965, v. 1175–1189
21. Hall, L A and Hinteregger, H E., *J. Geophys Res* , 1970, **75**, 6959–6965.
22 Timothy, A F. and Timothy, J G , *J Geophys Res* , 1970, **75**, 6950–6958
23. Hinteregger, H E , Bedo, D E. and Manson, J E , *Radio Sci.*, 1973, **8**, 349–359.
24 Torr, M R., Torr, D G., Ong, R A and Hinteregger, H E , *Geophys. Res Lett* , 1979; **6**, 771–774
25 Hinteregger, H E , *Adv Space Res* , 1981, **1**(12), 39–52.
26 Torr, M R. and Torr, D G , *J Geophys Res* , 1985, **90**, 6675–6678
27 Oster, L , *J Geophys. Res* , 1983a, **88**, 1953–1964
28 Oster, L., *J Geophys Res.*, 1983, **88**, 9037–9052
29. Rosenberg, T. J., Morris, P. B. and Lanzerotti, L. J., *Phys Rev Lett* , 1981, **47**, 1343.
30. Emmons, S , *Los Angeles Times*, 1979, p. cc-1, February 13
31. Goldberg, L., *Sci. Am* , 1969, **220** (6), 92–102.